

PACS numbers: 42.55.Wd; 42.60.Fc; 42.60.Gd
DOI: 10.1070/QE2012v042n09ABEH014959

Self-modulation oscillation regimes in fibre lasers with microoptomechanical resonance structures

F.A. Egorov, V.T. Potapov

Abstract. **Self-modulation oscillation regimes are studied in erbium fibre lasers with intracavity microoptomechanical structures (microoscillators) of different types, namely, based on silicon structures and consisting of special waveguide segments. Optical excitation of acoustomechanical vibrations of microoscillators is accomplished using photothermal effect or light pressure. Under the conditions of resonance interaction, i.e., when the eigenfrequencies of microoscillators coincide with the frequencies of relaxation oscillations or with those of intermode beats, the dependences of self-oscillation characteristics on the system parameters are found and the stability of the self-modulation frequency within 10^{-4}–10^{-6} is obtained at relatively low (40–300) *Q*-factors of microoscillators. The possibility to construct multivariate (multichannel) fibreoptical sensors of physical quantities with frequency division of measurement channels is demonstrated.**

Keywords: *relaxation oscillations, fibre laser, self-modulation, passive Q-switching, microoptomechanical resonance structure.*

13. Introduction

The studies of interaction between microoptomechanical resonance structures (MOMRSs) and laser radiation are one of the urgent issues of research and technology [1–3], within which the interdisciplinary studies joining micromechanics and fibre optics and aimed at the design of novel functional fibreoptical devices have been extensively developed in recent years. The key role in these devices is played by the MOMRS mechanical degrees of freedom, interacting with laser radiation.

MOMRSs (microoscillators) represent multifunctional structures having micron and submicron dimensions and fabricated using plasmachemistry or preferential etching of dielectric and semiconductor materials (glass, silica, silicon, etc.) [4], in which a fraction of optical radiation energy can be converted into acoustomechanical vibrations as a result of photoinduced MOMRS deformations, caused by photothermal effect, light pressure, electrostriction, photopiezoelectric effect in semiconductors and other mechanisms. The efficiency of conversion depends on a number of factors, namely, the characteristics of the light wave (spectral range, polarisation state, and modulation frequency), the physicochemical parameters of the materials, the construction and dimensions of MOMRSs, the external conditions, etc. In laser optical systems MOMRSs can operate as microminiature mirrors, deflectors, and optical waveguides, the characteristics of which are changed under the action of light. Being distributed oscillatory systems, microoscillators are characterised by a wide spectrum of eigenfrequencies and forms of elastic eigenmodes with pronounced resonance properties.

The introduction of a microoscillator into the feedback circuit of a laser may lead to passive modulation of laser radiation parameters with the modulation depth, essentially depending on frequency and demonstrating resonance behaviour at the frequencies of MOMRS eigenmodes. Of great interest are also systems with resonance interaction, in which the MOMRS eigenfrequencies coincide with characteristic frequencies of different processes in the laser (relaxation vibrations, intermode and polarisation beats, etc.), which may strongly affect the dynamics of laser oscillation. Satisfying the resonance interaction conditions may be relatively simple in fibre lasers (FLs), in which by variation of resonator parameters it is possible to control frequency-temporal and energy characteristics of laser radiation within wide limits. In the present paper the conditions for self-modulation regimes of FL oscillation in the presence of resonance interaction with various types of MOMRSs are considered.

14. Self-modulation in fibre lasers with MOMRSs under conditions of resonance with relaxation oscillations of laser radiation

Optical schemes of the studied erbium fibre lasers (EFLs) with MOMRSs are presented in Fig. 1. In the considered EFLs the role of MOMRSs is played by silicon structures with vibrational elements, implemented as micromembranes, microcantilevers or microbeams with various boundary conditions and the following characteristic dimensions: the diameter of membranes 500–150 μm, the thickness 2–20 μm; the length, width and thickness of microcantilevers and microbeams 100–150 μm, 10–200 μm, and 2–40 μm, respectively (Fig. 2). The eigenfrequencies f of fundamental modes of MOMRS acoustomechanical vibrations lie within the range of 3–450 kHz, the *Q*-factor of microoscillators (in air) Q = 40–300, and in vacuum conditions with residual pressure $p \simeq 10^{-2}$ Torr Q = 100–2000. The structures are fabricated by preferential etching of monocrystalline silicon, doped with boron, which allows creation of MOMRSs with various topologies. The deposition of metallic or dielectric films on the MOMRS surface allows formation of microoscillators with the required optical and other physical properties.

F.A. Egorov, V.T. Potapov V.A. Kotel'nikov Institute of Radio Engineering and Electronics, Russian Academy of Sciences, Fryazino Branch, pl. Akad. Vvedenskogo 1, 141120 Fryazino, Moscow region, Russia; e-mail: egorov-fedor@mail.ru;

Received 27 July 2012
Kvantovaya Elektronika **42** (9) 808–817 (2012)
Translated by V.L. Derbov

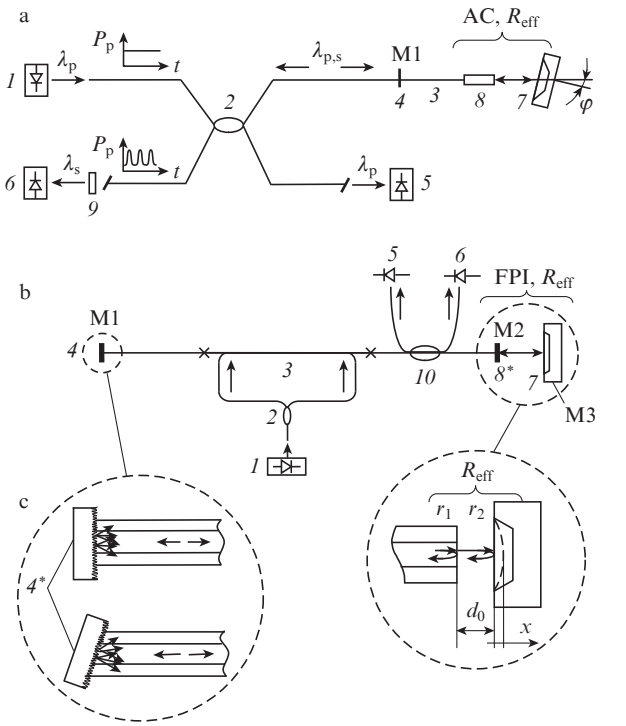

Figure 1. Schematic diagrams of lasers with a MOMRS and optical feedback via autocollimator (AC) (a) or Fabri–Perot interferometer (FPI) (b):
(*1*) laser pump diode (λ_p = 980 nm); (*2*) fibre multimode splitter; (*3*) active optical fibre; (*4*) dielectric semitransparent reflector, $R(\lambda_s) \simeq$ 20%–90%; (*4**) diffuse reflector (Fig. 1c); (*5*) and (*6*) InGaAs photodiodes; (*7*) MOMRS; (*8*) collimator (SELFOC); (*8**) outlet semitransparent mirror (multilayer interference reflector or boundary between the optical waveguide and air) (Fig. 1b); (*9*) optical filter; (*10*) fibre single-mode splitter (λ_s = 1.5 μm); (M1, M2, M3) reflectors; R_{eff} is effective reflection coefficient.

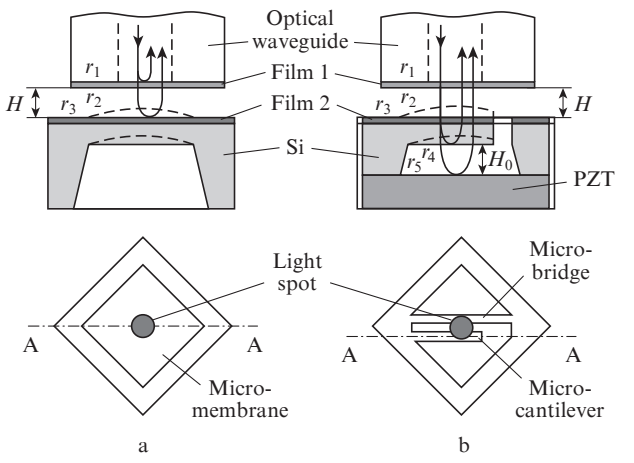

Figure 2. Schemes of MOMRSs based on micromembrane (a) and microcantilever (b); PZT is plumbum–zirconium–titanium piezoelectric ceramics.

In the studied EFLs the microoscillators are located at the exit of the fibre part of the laser and play the role of either a resonator mirror, or an additional external reflector. Double-clad active optical fibres (AOFs) are pumped using radiation of semiconductor lasers with the wavelength $\lambda_p \simeq 980$ nm. The optical feedback between the EFL and MOMRS is provided either by a MOMRS-based autocollimator (AC) or by a Fabry–Perot interferometer (FPI), formed by a semi-transparent reflector at the exit face of the EFL and the reflecting surface of the MOMRS, which makes a two- or three-mirror laser resonator, respectively.

The laser radiation incident on the MOMRS causes its photoinduced deformation, which in the case of positive feedback can lead to self-modulation of intensity and other parameters of the generated radiation at the frequency of MOMRS eigenmodes. The typical mean power of EFL radiation, incident on the MOMRS, is $\bar{P} \simeq 1-10$ mW.

The mathematical models of FL-MOMRS systems [5], based on the fibre laser rate equations for three-level (Er^{+3}, [6]) and four-level (Nd^{+3} [7]) schemes, as well as the equations of linear microoscillator in the single-resonance approximation, are considered and analysed in Refs [8,9]. The results of this analysis show that one of the basic conditions for self-oscillation in the system is the coincidence of the eigenfrequency of MOMRS mechanical vibrations with the frequency of relaxation oscillations in the FL, $f_{rel} \simeq f$. In particular, single-frequency synchronous oscillations of the microoscillator and laser radiation are possible under the conditions of continuous pumping in the considered system, which manifest themselves in self-modulation of the radiation intensity at the frequency of synchronous oscillations F, virtually coincident with the frequency of MOMRS eigenmode vibration ($F \approx f$).

The experimental studies were carried out mainly using erbium-yttrium fibre lasers (EYFLs). In the present work it is experimentally found that in the EYFL–MOMRS systems under the condition $f_{rel} \simeq f$ self-modulation is also possible in the schemes of lasers with so called nonresonance feedback [10], in which the role of one of the optical resonator mirrors (M1) is played by a diffuse light scatterer, such as chalk, paper, and sheets with a fine-grained (0.3–0.5 μm) rough surface used for grinding optical connectors (Fig. 1c). This fact means that for the existence of self-modulation regimes of this sort ($f_{rel} \simeq f$) the mode composition of laser radiation does not play a crucial role, and the character of the system behaviour may be described within the concept of radiation as a whole [11].

It is remarkable that the EYFL–MOMRS systems with the feedback via a SELFOC-based autocollimator (beam diameter 300–400 μm) demonstrated high stability with respect to the impact of destabilising factors [12,13], which is important in the design of high-precision frequency-domain sensors. Provided that the characteristics of the MOMRS and the EYFL optical resonator are given, the behaviour of the system is determined by the level of the EYFL pumping and the angle φ between the axis of the collimated beam and the normal to the MOMRS surface. In the space of the parameters mentioned, the region of excitation of self-oscillations possesses a rather complicated structure [13]. For creating fibreoptical sensors (FOSs), based on self-excited oscillations, of particular importance is the presence of areas with 'soft' excitation regime, in which reversible and stable (breakdown-free) self-oscillations with reproducible parameters take place. In these areas the relative fluctuations of the self-modulation frequency $\Delta F/f = |F-f|/f$ for the given MOMRS parameters do not exceed 10^{-4}. The dependence $F(f)$ is practically linear: within the range of relative variation of resonance frequencies $|\Delta f/f| \leqslant 5\%$ the nonlinearity coefficient does not exceed 0.1%.

In the present work it was also found that under the conditions of polarisation-isotropic pump of the EYFL, implemented by simultaneous focusing of two orthogonally polarised pump radiation beams with similar power on the AOW face, in the case of using a MOMRS with high temperature stability

$[f^{-1}(\Delta f/\Delta T) \simeq 2\times10^{-5}\,^{\circ}\mathrm{C}^{-1}]$, excited by light pressure, the short-time (during 1 hour) relative instability of self-modulation frequency under the normal conditions was $|\Delta F/F| \approx 2\times10^{-6}$ ($f \approx 60$ kHz, $Q \simeq 250$). This indicates the possibility in principle to create frequency-domain FOSs with wide dynamical range of measurements. Note that in the course of experiment no special measures were taken to protect (isolate) the system from external perturbations of the basic elements of the laser scheme, as well as to stabilise the parameters of the pump source. The relative fluctuations of the pump power $|\Delta P_p/P_p|$ amounted to ~3%, and ΔT was equal to 0.1 °C.

The possibility of using the resonance self-modulation regime for creating frequency-domain FOSs is confirmed by the data, presented in Fig. 3 that shows the dependences of the self-modulation frequency on the pressure and the temperature for a microcantilever MOMRS and a microbeam with supports on the membrane, respectively. The transformation function and the sensitivity of a temperature FOS can be varied within significant range, e.g., by coating the microoscillator resonator with a metallic film. The sensitivity of a pressure FOS can be varied by changing the thickness of the membrane. The experiments with combined MOMRSs, containing the films of magnetostrictive materials (Ni, Fe) and MOMRSs, mounted on piezoelectric lead zirconate titanate substrates, demonstrated the possibility to create a frequency-domain FOS of steady-state (quasi-static) electric and magnetic fields.

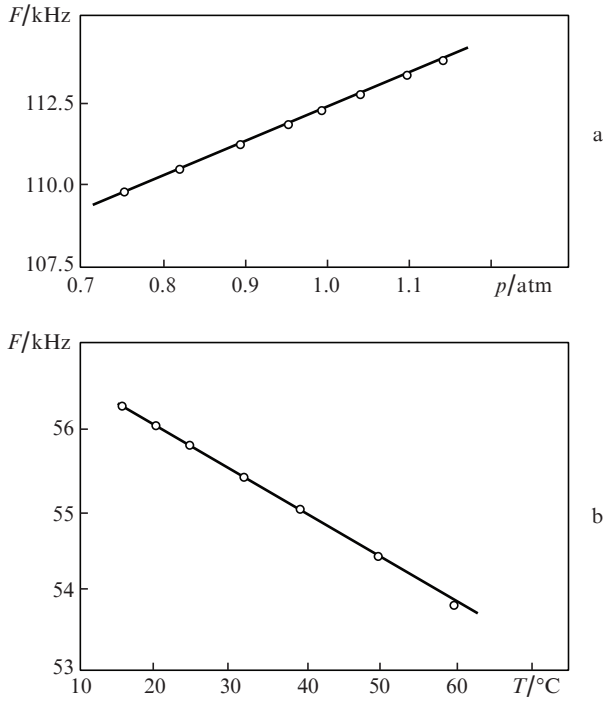

Figure 3. Dependences of the self-modulation frequency on the pressure (MOMRS is a microbridge on the membrane) (a) and on the temperature (MOMRS is a microconsole) (b).

15. Resonance self-modulation of EYFL intensity under passive mode locking using MOMRS

The relatively large length of fibre EYFL cavities ($l \gtrsim 1$ m), leading to sufficiently large lifetimes of photons, as well as considerable inertia of the laser active medium, with the limitations of the pump power taken into account, yield the frequency of EYFL relaxation oscillations f_{rel}, as a rule, not exceeding 300 kHz. Therefore, in the case of using high-frequency microoscillators ($f \gtrsim 500$ kHz) it is difficult to implement the considered mechanism of self-oscillation excitation. At the same time, thanks to considerable spectral width of the EYFL active medium amplification band that amounts to 30 nm and greater, the oscillation of the EYFL can be implemented in the multimode regime with the frequency separation between the modes $\Delta\nu \cong c/(2nl)$, where c is the speed of light in vacuum; n is the refractive index. In this case, the variation of the resonator length allows implementation of the resonance condition of another type, $\Delta\nu = f$, under which the efficient interaction between EYFL and MOMRS is possible in a wider range of microoscillator frequencies. Figure 4 shows a schematic diagram of the experimental setup for investigating such interaction [14].

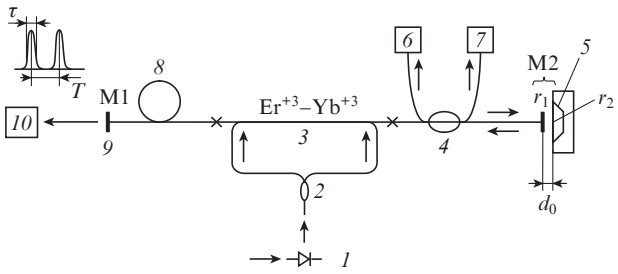

Schematic diagram of the fibre laser with external microresonator reflector:
(*1*) laser pump diode (λ_p = 980 nm); (*2*) fibre multimode splitter; (*3*) active optical fibre; (*4*) fibre single-mode splitter; (*5*) MOMRS; (*6*, *7*, *10*) photodetectors; (*8*) segment of SMF-28 fibre; (*9*) dielectric mirror [$R(\lambda_s) = 90\%$].

The optical length of the fibre laser resonator could vary both discretely and continuously, at the expense of introducing passive waveguide segments and smoothly heating them. The multilayer interference mirror M1 is formed directly on the face of the optical waveguide. The mirror M2 represents an optically-tunable FPI, formed by the reflecting face of the silica waveguide with the reflection coefficient $r_1 \simeq 3.5\%$ and the reflecting surface of the MOMRS ($r_2 \approx 70\%$) having the form of a microbridge with the eigenfrequency of the bending vibration fundamental mode $f_1 \approx 370$ kHz. The FPI base is expressed as $d = d_0 + y$, where d_0 is the initial value of the base with the EYFL switched off; y is the shift of the MOMRS due to photoinduced deformation. Tracing of the EYFL oscillation dynamics and the state of microoscillator vibrations was implemented using fast photodetector devices (*6*, *7*, *10*).

Under the resonance conditions ($\Delta\nu = f_1$), corresponding to $l \approx 280$ m, at certain values of the FPI base, belonging to definite branches of interferograms, the fibre laser becomes switched over to the regime of regular pulse generation with the pulse repetition rate F, close to the mode frequency separation ($F \approx \Delta\nu$). The transition to the mentioned regime of oscillation has a pump level threshold, and with the growth of pump power the duration of pulses decreases (the minimal duration achieved is $\tau_{min} \approx T/30$, $T = F^{-1}$), while the laser intensity modulation depth grows, approaching 100%. The mentioned regularities are typical for the regime of passive mode locking in lasers. Figure 5 shows the self-oscillation frequency F versus the relative variation of the fibre resonator

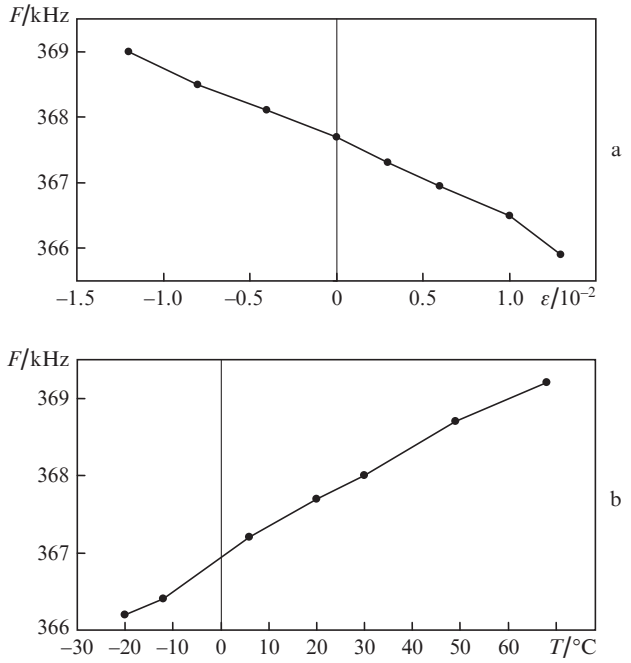

Figure 4. Dependences of the pulse repetition rate F on the relative variation of resonator length $\varepsilon = \Delta l/l$ (a) and MOMRS temperature (b).

length of the EYFL and the temperature of the MOMRS, which demonstrates the possibility to use this regime in frequency-domain FOSs.

Note that the self-oscillations at the MOMRS eigenfrequency f_1 = 370 kHz are efficiently excited also under the multiple-resonance conditions ($\Delta\nu = {}^1\!/_2 f_1$), easily attainable by doubling the length of the laser resonator, $l_2 = 2l_1 \approx 560$ m.

The ratio of calculated values of the eigenfrequencies for three lowest vibrational modes of the considered MOMRS looks as $f_1 : f_2 : f_3 = 4.73 : 7.85 : 10.99$ [15], from which it follows that $f_3 = (10.99/4.73) f_1 \approx 860$ kHz. The antinodes for the first and the third modes of the transverse vibrations are concentrated in the centre of the microoscillator. Therefore, if the laser radiation is focused onto the microoscillator centre, one can expect that by the appropriate change of the EYFL resonator length it is possible to provide the conditions for exciting self-oscillations also in the third eigenmode with the frequency $F \approx f_3$.

The experiment completely confirms this expectation: the self-oscillations in the EYFL–MOMRS system with the frequency $F \approx f_3^{\text{exp}} \approx 899$ kHz are observed in correspondence with the resonance condition $\Delta\nu \approx f_3$ at the resonator length $l_3 \approx (f_3/f_1) l_1 \approx 110$ m.

In contrast to the self-oscillations under the conditions of resonance with relaxation oscillations, whose maximal frequency in 'common' EYFLs does not exceed $f_{\text{rel}} \simeq 300$ kHz, in the considered system the limits of possible MOMRS resonance frequencies are essentially wider. Thus, for the EYFL optical resonator length $l \simeq 1$ m, the eigenfrequency f of the microoscillator vibrations may achieve the value of $\Delta\nu$ and amounts to ~100 MHz.

Since the MOMRS vibrations change both the amplitude and the phase of the light wave, reflected from FPI, the observed regime of passive mode locking can be caused by modulation of both the Q-factor and the phase in the laser resonator [16]. Note, that an important role in the dynamics of EYFLs with a 'high-frequency' MOMRS may be played by the Doppler frequency shift of light, reflected from the moving surface of the MOMRS ($\Delta\nu_{\text{D}} = \nu_0 2v/c$), the influence of which may increase when approaching the condition of other type of resonance, $\Delta\nu_{\text{D}}^{\max} \simeq f \simeq \Delta\nu$. The maximal value of the Doppler frequency shift is determined by the maximal velocity of the microoscillator $v_{\max} = 2\pi f A$, $A \simeq \lambda_s/4\pi$ being the amplitude of vibration. The peculiarities of FL oscillation under such conditions require further studies.

In connection with the possibility of simultaneous generation of orthogonal polarisation supermodes in fibre lasers, it is interesting to study the dynamics of fibre lasers with the MOMRS based on integral optical waveguides, in which the photoinduced forces, leading to MOMRS deformation, depend on the polarisation state of the propagating radiation [17]. Due to the dependence of the polarisation dispersion in the integral optical waveguide on the photoinduced deformations the effects of locking between the polarisation beats of FL supermodes and the microoscillator vibrations become possible.

Note that in a fibre laser it is rather simple to satisfy the condition $\Delta\nu \simeq 0.1 - 100$ MHz; this interval covers the region of resonance frequencies for a variety of MOMRSs, used, in particular, as sensitive elements of frequency-domain FOSs. It is of great interest to study the considered regime in fibre lasers with resonators based on special strong-dispersion optical waveguides. This is expected to increase the allowed range Δf of tuning the resonance MOMRS frequency at a fixed resonator length at the expense of the shift $\Delta\lambda_s$ of the generated radiation spectrum in correspondence with the resonance condition $\Delta\nu + D l \Delta\lambda_s \simeq f + \Delta f$, D being the optical waveguide dispersion. The considered regime may be used for investigating the properties (mechanical, acoustical, optical, etc.) of micro- and nanoobjects and microstructured (special) optical fibres.

16. Fibre laser with passive mode locking based on photoinduced resonance vibrations of optical waveguide

In the EYFLs considered above the construction of exploited MOMRSs essentially complicates the problem of providing efficient and stable optical connection with the fibre part of the laser resonator, particularly, under the impact of destabilising factors, which requires special technological solutions. In this connection it is of considerable interest to investigate self-modulation processes in FLs based on of all-fibre schemes, in which the MOMRS represents a segment of a special fibreoptical waveguide [18]. Figure 6 shows the schematic diagram of EYFL with a passive Q-switch based on a segment of special optical fibre with large size of the lowest mode LP_{01}, executing transverse resonance vibrations under the impact of laser radiation.

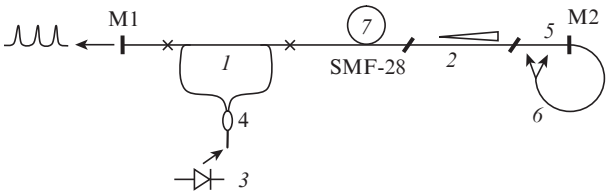

Figure 5. Schematic diagram of the fibre laser with a passive Q-switch: (*1*) active optical fibre (Er^{+3}–Yb^{+3}); (*2*) mode expander with a conical waveguide; (*3*) laser pump diode (λ_p = 980 nm); (*4*) fibre splitter; (*5*) vibrating segment; (*6*) auxiliary optical waveguide 100/125 μm; (*7*) additional segment of SMF-28 fibre; (M1, M2) semitransparent reflectors.

The schematic diagram and parameters of the elements of the passive fibre Q-switch on the basis of a metallised multimode stepwise optical fibre (MMSOF) are presented in Fig. 7. The total length of the MMSOF segment coated with copper is $l \approx 35$ mm, the length of the vibrating section being $l_{osc} \approx 9$ mm. The faces of the MMSOF, embedded in ceramic capillaries, are polished and processed up to the optical surface finish class. One end is coated with a semitransparent interference reflector, the EFL resonator mirror, and the other end serves to provide an efficient optical connection with the mode expander. The parameters of the MMSOF are as follows: the numerical aperture NA = 0.2, the core diameter $d_c \approx 100$ μm, the diameter of silica cladding $d_{out} \approx 125$ μm (the thickness of the copper coating $h \approx 10$ μm), the characteristic parameter of the MMSOF $V \approx 41$. In correspondence with the formula $d_m = (2 \ln V)^{-1/2} d_c$, the diameter d_m of the fundamental mode LP_{01} [19] amounts to ~37 μm, which is close enough to the diameter of the mode at the exit of the mode expander used (42 μm).

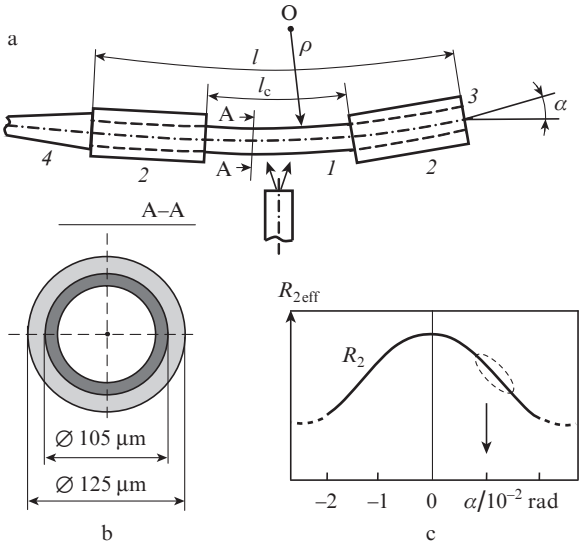

Figure 6. Schematic diagram (a) and parameters (b) of the fibre Q-switch and dependence of the effective reflection coefficient on the bending angle (c):
(*1*) vibrating segment; (*2*) ceramic capillaries (ferrules); (*3*) interference semitransparent mirror; (*4*) conical waveguide (mode expander); ρ is the bending radius.

The given MMSOF construction simultaneously provides the required efficiency of excitation of bending acoustomechanical vibrations, sufficiently high resonance frequency, and Q-factor of a fibre microoscillator. The optical excitation of vibrations is achieved mainly due to photothermal effect. The EYFL radiation is directed to the surface of the vibrating segment by means of the auxiliary multimode stepwise waveguide (100/125 μm). To enhance the absorption of the radiation, the metallic surface of the optical waveguide was coated with a thin layer of smoke black.

In the EYFL oscillation regime, provided that the resonance condition $f_{rel} \approx f$ is satisfied and the output radiation power, a part of which is incident on the surface of the vibrating segment, exceeds a certain threshold value ($P \geqslant 4$ mW), the self-modulation of intensity at the frequency $F \approx f$ is observed. The modulation arises, if the surface of the MMSOF is illuminated from only one definite side, providing positive feedback in the self-oscillatory system considered. A relatively low frequency of EYFL relaxation oscillations (f_{rel} = 5–10 kHz), together with the necessary level of the output radiation power ($P \geqslant 4$ mW), was achieved at the expense of increasing the laser resonator length by means of an additional SMF-28 fibre segment 120 m long. Thanks to small bending of the MMFOS (the angle $\alpha \lesssim 1°$) the resonance frequency of the vibrating section may be efficiently controlled at the expense of longitudinal deformations, which will allow the usage of such elements as frequency convertors in fibreoptical sensors of physical quantities.

Figure 8 shows the experimental dependence of the resonance frequency f_0 of the vibrating section on the tension deformation $\varepsilon = \Delta l_{osc}/l_{osc}$, obtained in the regime of induced oscillations, and the temperature dependence of the self-modulation frequency $F(T)$ and intensity of the EYFL with the abovementioned fibre Q-switch, fixed at a copper substrate with variable temperature. The growth of the substrate temperature leads to stretching of the vibrating section, which causes the increase in self-modulation frequency with increasing temperature: $F^{-1}(\Delta F/\Delta T) \approx 0.4\%\ °C^{-1}$.

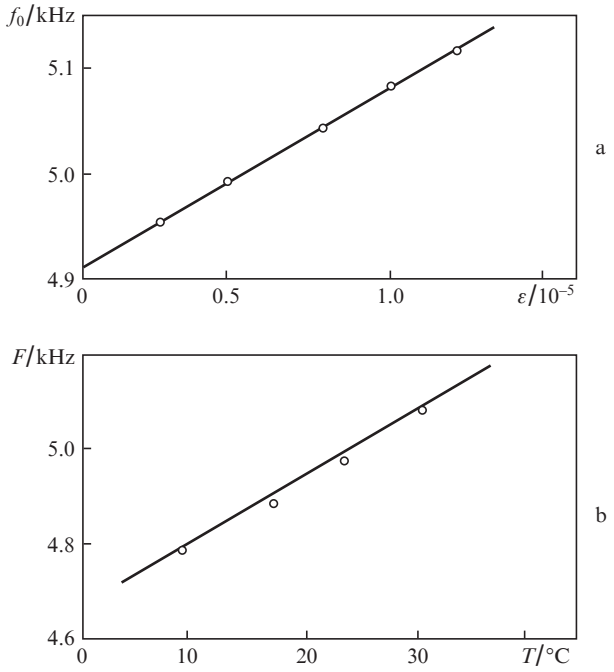

Figure 7. Dependences of the resonance frequency on the deformation (a) and of the frequency of self-modulation oscillations on the temperature (b).

Along with high efficiency, the proposed method of passive Q-switching, based on mode transformation in optical waveguides, is characterised by spectral uniformity of losses in the range of wavelengths 1520–1570 nm, which softens the requirements to spectral stability of EYFL laser radiation. Note, that in MMFOSs having the structure of a homogeneous core with a metallic cladding (including hollow metallic waveguides) the photothermal deformations may be caused by the absorption of radiation in the metallic layer directly at the inner boundary between the core and the cladding without any additional auxiliary optical waveguides. In this case the bending photoinduced deformations and vibrations may be excited due to asymmetry of the cross section of the metallic cladding, which essentially simplifies the scheme of the FL.

Thus, in a fibre laser the regime of passive Q-switching is implemented, based on photoinduced resonance vibrations of the waveguide segment, which is simultaneously an optical element of the laser resonator. The additional simplification of the all-fibre laser scheme may be achieved by combining the functions of the vibrating section and the active waveguide within a single optical fibre element. Here, as we expect, an optimal way is to use FLs based on single-mode active optical fibres with large mode diameter [20], which is also favourable to the increase in efficiency of converting laser radiation energy into acoustomechanical vibrations of the MOMRS. The proposed scheme may serve as a basis for designing frequency-domain sensors of linear deformations. These devices are optical analogues of the well-known electromechanical string sensors of deformations [21], differing from the latter by the absence of any electric schemes or circuits in the measurement zone, which is undoubtedly favourable to widening the area of their application.

An important role in improving the construction and characteristics of optical fibre passive MOMRS-based modulators may be played by recent achievements in the field of microstructured and photonic-crystal optical waveguides, which, from the point of view of elasticity theory, are acoustic waveguides with complex structure [22]. In these waveguides the photoinduced vibrations of various structure elements can be excited, leading to modulation of optical characteristics of propagating radiation [23]. Using inertialess photoinduced deformation mechanisms of nonthermal nature, i.e., the 'gradient' forces [17] and electrostriction [24], caused by transverse gradients of the light wave intensity in these optical waveguides (including integral and optical waveguides on the basis of composite electrostriction materials [25]), an essential increase in efficiency and resonance frequencies of fibreoptical MOMRSs is possible.

17. Parametric oscillations of optical micronanofibres in the process of propagation of laser radiation

Micronanofibres (MNFs) with transverse dimensions not exceeding the wavelength of light ($a/\lambda \leqslant 1$) possess many unique properties that allow creation of fibreoptic elements and devices of new generation with advanced functional capabilities [26]. The MNFs can be made of various dielectric and semiconductor materials, providing a wide scope of properties and regimes of operation of the fibreoptic elements. Depending on the material optical properties, shape and dimensions of the MNF, different regimes of radiation propagation are possible: when $V \leqslant 2$ the main part of the guided mode propagates beyond the nanofibre, while at $V \gg 2$ the radiation is concentrated within it.

In the field of a light wave at $V \leqslant 2$ and asymmetric distribution of the propagating radiation intensity with considerable transverse gradient the fibre is subjected to the 'gradient' ponderomotive force [17]. If the radiation is modulated, this force gives rise to bending vibrations of the MNF, which possess resonance character at the modulation frequencies f, close to the eigenfrequencies of the MNF Ω ($\Omega \simeq f$). In photonic-crystal MNFs the resonance frequencies of optically excited vibrations Ω can be as large as 3 GHz [23]. Such MNFs may serve as a basis for a new class of optically controlled fibre elements, including MOMRSs.

We considered the possibility of implementing an alternative mechanism of optical excitation of micronanofibres vibrations, which is efficient under the condition $V \gtrsim 2$. In this case almost all of the exciting modulated radiation propagates within the uniform transparent MNF, in which the abovementioned 'gradient' mechanisms appear to be inefficient. In the present case the excitation of vibrations occurs under the conditions of parametric resonance, caused by the dynamic instability of the MNF in the course of modulated radiation propagation; the maximal amplitude of vibrations is achieved under the conditions of the principal parametric resonance $f = 2\Omega$. Due to the dependence of the resonance frequency on various external perturbations and environment parameters, the MNFs-based MOMRSs may be used as sensitive elements in frequency-domain FOSs of physical quantities [27]. Figure 9 displays a segment of an optical fibre with a micronanofibre section of the simplest type and the scheme, by means of which it is possible to excite and register the MOMRS parametric oscillations. To increase the sensitivity of the scheme, the MNF segment is placed in the Fabry–Perot resonator, formed by semitransparent reflectors with the reflection coefficients $R_{1,2}$. The abovementioned MNF may be fabricated using the redraw process in scanning flame [26] applied to a standard SMF-28 fibre, which allows variation of the MNF dimensions within wide limits.

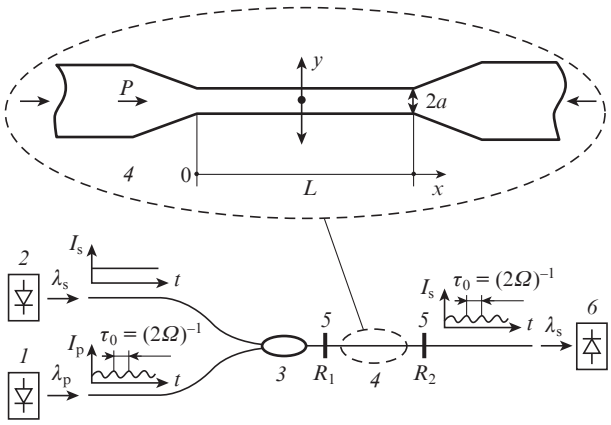

Figure 8. Schematic diagram of exciting MNF parametric oscillations: (*1*) source of intensity-modulated exciting light (λ_p); (*2*) source of cw coherent probe radiation (λ_s); (*3*) fibreoptic multiplexor; (*4*) fibre segment with a nanowaveguide section; (*5*) intrafibre reflectors; (*6*) photodetector device.

The considered MOMRS represents an oscillatory system with distributed parameters in the form of an elastic rod with rigidly fixed ends. At static bending and transverse vibrations of the MNF the bended segments, in which the change of the light momentum occurs, are subjected to transverse forces from the field of propagating radiation. The distribution of arising forces may be approximately determined using the approach, based on the certain analogy between an optical fibre and a pipe with flowing liquid [28]. This approach is correct if the power of radiation is conserved along the MNF and the direction of the radiation momentum coincides with the waveguide axis. For the nanowaveguide bending radius $R \gg R_{cr} \cong 3aV^2/(4\mathrm{NA}^2W^3)$ the distortions in the distribution of the mode field in the bended segment are insignificant [19], for silica MNF with a = 500 nm, NA = 1, and λ = 1000 nm the critical radius R_{cr} = 30 μm (W being the parameter of intensity distribution in the cladding). Restricting ourselves to the initial stage of excitation of the fundamental type of MNF bending vibrations, we can show that for the MNF dimension $L \geqslant 2\sqrt{2}a/\mathrm{NA}$ the condition $R \gg R_{cr}$ is satisfied liberally for

vibration amplitudes $A \leqslant a$. In MNFs with the dimension $L \leqslant 10$ mm and $a \geqslant 300$ nm the power losses do not exceed 5%, so that, in correspondence with the proposed model, the equation of motion for MNFs has the form [29]

$$\rho_s s \frac{\partial^2 y}{\partial t^2} + \frac{2P}{c^2}\frac{\partial^2 y}{\partial t \partial x} + \left(N + \frac{P}{c}\right)\frac{\partial^2 y}{\partial x^2} + EJ\frac{\partial^4 y}{\partial x^4} = 0 \qquad (1)$$

with the boundary conditions $y|_{x=0,L} = 0$, $y'|_{x=0,L} = 0$, where $y(x,t)$ is the transverse displacement of the MNF axial line; $s = \pi a^2$; $J = \pi a^4/4$; E and ρ are the Young modulus and the material density of the MNF; c is the speed of light in the nanofibre; P is the radiation power in the MNF. The total density $\rho_s = \rho + \rho_r$, where $\rho_r = P/sc^3$ is the equivalent ('mass') density of light ($\rho_r \ll \rho$); N is the applied longitudinal force of MNF compression (tension); $N + P/c = N^*$ is the effective longitudinal force.

The analysis of Eqn (1) shows that for constant radiation power, exceeding a definite (critical) value, the rectilinear shape of the MNF is unstable (Euler instability), which leads, particularly, to the static bending of the MNF.

In the case of modulated power $P(t)$ Eqn (10) describes an oscillatory system with parametric excitation, in which a parametric resonance is possible, leading to the excitation of MNF oscillations. Assuming that $P(t) = \bar{P}(1 + m\cos\omega t)$, where $\bar{P}$ is the mean power; m is the modulation depth; $\omega = 2\pi f$ ($|f/2\Omega - 1| \ll 1$). Using the Bubnov–Galerkin method [30], we find that under the condition $\Omega \ll c/L$ the contribution of the second term in Eqn (1) can be neglected. As a result, we get the equation, describing parametric oscillations:

$$\ddot{T} + \frac{\Omega}{Q}\dot{T} + \Omega^2\left[1 - \frac{\bar{P}}{P_*}(1 + m\cos\omega t)\right]T = 0, \qquad (2)$$

where

$$P_* = EJc\int_0^L \varphi\frac{a^4\varphi}{\mathrm{d}x^4}\mathrm{d}x\left(\int_0^L \varphi\frac{a^2\varphi}{\mathrm{d}x^2}\mathrm{d}x\right)^{-1};$$

$\varphi(x)$ is the shape of MNF vibrations; $y(x,t) = \varphi(x)\,T(t)$. The second term in Eqn (2) accounts for damping of MNF vibrations that is characterised by the Q factor. Neglecting the difference between the MNF bending shapes caused by eigenmode oscillation and by Euler instability, we get $P_* = cN^*_{cr}$. In the system, described by Eqn (2), at $f = 2\Omega$ and the values of the excitation coefficient $\mu = \bar{P}m/2(P_* - \bar{P})$, exceeding the threshold value $\mu_{cr} = Q^{-1}(1 - \bar{P}/P_*)^{1/2}$, the principal parametric resonance is observed, when the amplitude of vibrations is limited by the nonlinear properties of the system only [30]. Thus, at $\bar{P} > \bar{P}_{cr} \cong 2\pi^3 cEa^4/(mQL^2)$ and $f \approx 2\Omega$ the resonance vibrations of the MNF with the frequency $f/2 \approx \Omega$ are excited. The Q factor of the vibrating nanosection depends on the parameters of the environment [31]; thus, under the normal conditions $Q \cong 10$–100, while in vacuum $Q \geqslant 10^4$. For MNF in vacuum with the dimensions $a = 500$ nm, $L = 3$ mm we get $\bar{P}_{cr} \cong 1$ mW. In this case, the radiation intensity in the MNF $I = \bar{P}_{cr}/s \cong 4\times10^9$ W m^{-2}, which is essentially lower than the threshold, limiting the light intensity in silica fibres [32].

The considered vibration mechanism is universal, practically inertialess and does not impose strict limitations on the MNF material properties. Note, that in strip and polymer micro-nanowaveguides [26], because of small thickness and relatively small elasticity modulus of the material, the transverse rigidity (EJ) is considerably smaller than in the considered silica nanofibres; therefore, in these waveguides the effects of static and dynamic instability, caused by the light propagation, may manifest themselves at $\bar{P} \ll 1$ mW. Significant optical powers ($\bar{P} \gg 1$ mW) take place, e.g., in nanofibre lasers [33] or in optically nonlinear MNFs in the regime of supercontinuum generation [34].

In fibre lasers based on optical nanowaveguides the instabilities are possible due to an alternative mechanism, namely, the longitudinal deformations of the laser resonator produced by the light pressure on the mirrors, which for a nanowaveguide laser resonator may be estimated as $\varepsilon = \Delta L/L \cong 2\bar{P}/(cEs)$ (we assume that the reflection coefficients $R_{1,2} \cong 1$). These deformations may lead to unstable laser oscillation, associated with excitation of longitudinal MNF vibrations with resonance frequencies Ω^* [35]. Combined longitudinal–transverse resonances are also possible ($\Omega \cong \Omega^*$) that additionally complicate the behaviour of the MNF. Therefore, in a number of cases the optical properties of MNFs with laser radiation should be determined as a result of solving a self-consistent problem with the arising vibrations taken into account. For standard fibres (SMF-28) the transverse rigidity exceeds the values, typical of MNFs, by eight orders of magnitude; therefore, in conventional fibres the abovementioned effects virtually do not manifest themselves.

In Eqn (2) $\Omega = \Omega(N,\bar{P}) = \Omega_0(1 - N^*/N^*_{cr})^{1/2}$, and the relative variation of the MNF vibration eigenfrequency, caused by the propagating radiation, is $\Delta\Omega/\Omega_0 \cong L^2\bar{P}/(8\pi^2 Esc)$. Therefore, in high-precision measurements of the MNF resonance frequency a limitation of the acceptable level of the laser radiation mean power fluctuations in the optical nanowaveguide arises. On the other hand, the dependence $\Omega(\bar{P})$ allows the resonance frequency control by varying the mean power of radiation in the MNF. The amplitude and the phase of MNF vibrations may be determined by using interferometric schemes (Fig. 10) that allow fabrication of FOSs on the basis of MNFs

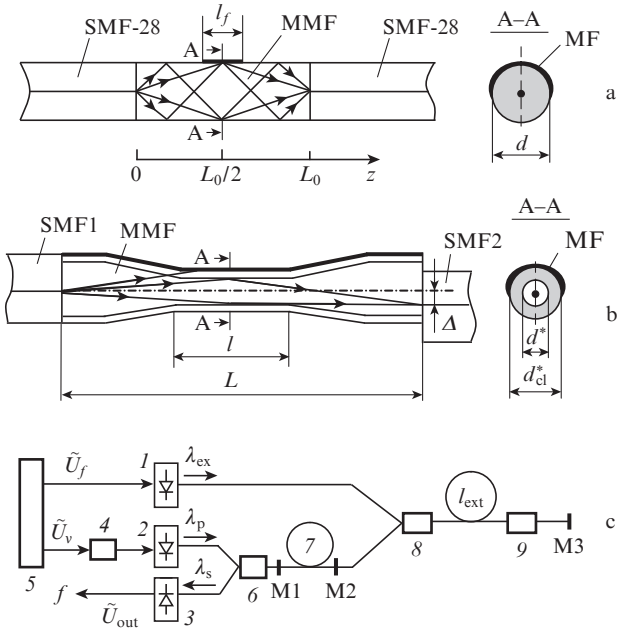

Figure 9. Schematic diagrams of optical waveguide structures SMS1 (a), SMS2 (b), and the measurement setup (c):
(*1*) source of exciting modulated radiation (λ_{ex} = 1480 nm); (*2*) laser pump diode (λ_p = 980 nm); (*3*) photodetector; (*4*) phase shifter; (*5*) generator of sinusoidal signals; (*6*) fibreoptic multiplexor (WDM) (980/1550); (*7*) fibre laser; (*8*) WDM (1480/1550); (*9*) SMS structure; (M1, M2, M3) selective semitransparent reflectors.

in all-fibre implementation, which is technologically rational for production and provides high performance characteristics. The studies of the dynamics of laser radiation in the MNFs with console fixing are also of great interest. In analogy with the behaviour of a console-fixed elastic pipe duct under the conditions of following load [36], the self-oscillations in MNFs are possible.

18. Photoinduced vibrations in MOMRSs based on irregular optical fibres

Interference effects in fibre structures based on single-mode (SMFs) and multimode (MMFs) fibres (SMS structures) open the possibilities to create a new class of fibreoptical devices [37–39]. Rather promising seem the studies aimed at creating optically controllable SMS structures, particularly MOMRSs, based on amplitude–phase modulation of radiation as a result of photoinduced acoustomechanical vibrations in SMS structures.

In the present Section we present the results of study of two types of SMS structures (Fig. 10a, b), namely, SMS1 with a multimode segment based on a uniform silica rod and SMS2 based on a silica stepwise fibre with biconical links (waists).

The photothermal excitation of the MMF segment is implemented at the expense of the energy of modulated radiation, propagating through it, a part of which is absorbed by the metallic film (MF) asymmetrically coating a fragment of the segment surface. Due to thermoelasticity, periodical mechanical stresses and bending moments appear in the segment, giving rise to vibrations [40]. In SMS1 structures the film is deposited on a small area in the middle of the segment. In SMS2 structures the film coats a half of the waist surface along the full its length; in this case the part of radiation, passing from the core into the cladding, is absorbed. In SMS1 the presence of the film also leads to an additional phase shift $\Delta\varphi_0$ for the rays, reflected from the boundary between the rod and the film.

From the transmission spectra $T(\lambda)$ of the studied structures SMS1,2 (in the range 1400–1600 nm) it is seen that the maximal values of transmission are $T_{\max} = 15\%–45\%$, the position $\lambda_{\max}$ and the value $T_{\max}$ being very sensitive to the parameters of the MMF segments: in SMS1 at fixed dimensions of the segments the values of $T_{\max}$ and $\lambda_{\max}$ depend on the thickness and the optical constants of the metallic film, and in SMS2 the crucial characteristics are those of the initial multimode fibre and the dimensions of the waist (L, l, d^*). For the principal interference maximum of transmission the half-maximum spectral widths $\Delta\lambda_{1/2}$ for the considered SMS1,2 amount to 8–20 nm. Note that in the SMS structures based on regular MMF segments the maximal absorption takes place for the segment length $L_k = L_0 k$, where $L_0 = 4nd^2/\lambda$; d and n are the diameter and the refractive index of the MMF core, respectively; λ is the wavelength of light; $k = 1, 2, \ldots$ [37]. In the MMF cross sections with the coordinates $Z_k = L_0(k - 1/2)$ the radiation is completely concentrated in a narrow belt at the segment surface, which provides efficient interaction of radiation in SMS1 structures with the small-size metallic film.

With multiple-beam interference taken into account, the radiation intensity in the receiving waveguide is determined by a superposition of resulting amplitudes of pairwise symmetric beams, propagating in the MMF segment along definite zigzag lines (trajectories), forming symmetric interferometer arms that converge in the light-guiding cores SFM1,2. The transmission maxima of SMS structures correspond to certain lengths L_k of the segment that provide formation of the maximal number of in-phase (to 2π) beams of the mentioned type. In axially symmetric SMS structures, because of quadrature condition violation (due to in-phase arms), these interferometers are characterised by low sensitivity to bending vibrations of the MMF segment. In the considered SMS1 structures the necessary sensitivity to the vibrations is achieved via phase unbalancing between the arms due to the additional phase shift $\Delta\varphi_0$ acquired by beams, reflected from the metallic film and forming one of the interferometer arms. To eliminate the interaction of the beams in the opposite arm of the interferometer with the metallic film the length of the latter is limited by the condition $l_f \lesssim 2nd/\mathrm{NA}$. The use of special film structures, in principle, allows providing maximal sensitivity of the interferometers ($|\Delta\varphi_0| = \pi/2$) [41]. Thus, in SMS1 the metallic film plays two important roles: provides the mechanism of optical excitation of MMF segment vibrations and determines the position of the operating point of the interferometers, allowing registration of small vibrations. In SMS2 the necessary sensitivity of the MMF segment to bending vibrations is achieved by optimisation of the operating point of the interferometers by transverse displacement of one of the SMS optical waveguides with respect to the MMF segment, i.e., axis misalignment of the SMS2 structure (Fig. 10b). The optimal transverse displacement Δ is determined experimentally and amounts to 1–3 μm. In the studied structures the films of nickel (Ni) and chrome (Cr) were used having the thickness of 50–200 nm, obtained by means of the method of electron-beam evaporation and characterised by good adhesion to the silica glass.

Schematic diagram of the setup for investigating the photoinduced vibrations of the SMS1,2 structures is presented in Fig. 10c. The optical excitation of the induced MMF segment vibrations was performed by means of the modulated radiation with the wavelength $\lambda_{ex} \simeq 1480$ nm, and the registration of the vibrations was implemented using a EYFL with diode pumping ($\lambda_p \simeq 980$ nm) that provides smooth controlling and harmonic modulation of the pump radiation power $P(t)$ by changing the supply current of the diode. The selective semitransparent reflector M3 at the outlet face of SMF2 provides almost complete reflection (93%) at the line of FL oscillation ($\lambda_s \simeq 1538$ nm) and transmission (87%) at the wavelength 1480 nm. Due to the optical connection of the EFL with the external resonator (M2–M3), comprising the SMS structure, the modulation of losses $\Delta\tilde{T}$ and phase $\Delta\tilde{\varphi}$ of the light wave in the SMS structure, caused by vibrations of the MMF segment, leads to the modulation of the FL output power [42]:

$$\frac{\Delta\tilde{W}}{W} = \frac{[\gamma_{\mathrm{rel}}^2 + f^2]^{1/2}}{[(f_{\mathrm{rel}}^2 - f^2) + \gamma_{\mathrm{rel}}^2 f^2]^{1/2}} F_{\mathrm{m}}(\Delta\tilde{T}, \Delta\tilde{\varphi}), \tag{3}$$

where $f_{\mathrm{rel}}(P)$ is the frequency of FL relaxation oscillations, depending, in particular, on the pump power P; f is the frequency of MMF segment vibrations; γ_{rel} is the damping parameter of the EFL relaxation oscillations; $F_{\mathrm{m}}(\Delta\tilde{T}, \Delta\tilde{\varphi}) = G(A)$ is the function of loss and phase modulation in the external resonator (M2–M3), depending, in turn, on the amplitude A of the MMF segment vibrations. In Eqn (3) it is assumed that the length of the external resonator $l_{\mathrm{ext}} \ll c/2f$.

In the experiment the resonance frequencies of fundamental vibration modes of the MMF segments with rigid fixation of the ends amounted to 4–15 kHz, the Q-factor of the mechanical vibrations (in air) was equal to 100–400; the length of the oscillating MMF segment was equal to a definite fraction of the multimode segment ($l/L_0 = 1/6–1/3$). The relatively low

frequencies of relaxation oscillations ($f_{rel} \leqslant 10$ kHz) were achieved via increasing the laser resonator length (M1–M2) by attaching a passive segment of the SMF-28 fibre to the active segment of the optical waveguide. The length of the external resonator is $l_{ext} = 10–20$ m. In correspondence with Eqn (3) the sensitivity of the EYFL to the vibrations of the MMF segment demonstrates resonance behaviour with the maximum at $f_{rel} \simeq f$, which is achieved by smoothly controlling the level of EYFL pumping.

Additional enhancement of sensitivity is possible via the use of nonlinear properties of lasers with modulated pumping [43]. In particular, we studied the possibility to increase the sensitivity of the EYFL at the expense of parametric amplification under the conditions of the principal parametric resonance, taking place at $\nu \simeq 2f_{rel} \simeq 2f$, where ν is the EFL pump power modulation frequency. Optimisation of the pump modulation depth $\Delta\tilde{P}/P \simeq 3\times10^{-2}$ and the phase difference $\Delta\Phi_{f,\nu}$ between the control harmonic signals $\tilde{U}_f$ and $\tilde{U}_\nu$ ($\nu = 2f$) in the given scheme allowed the sensitivity increase by 10%–13%. The estimates show [44] that the optimisation of the scheme parameters would provide an opportunity to increase the sensitivity of the fibre laser at least by 2–3 times at the expense of parametric amplification of signals. It is important to emphasise that the high sensitivity of the FL allows registration of MMF segment vibrations with small amplitude ($A \ll d$), which significantly reduces the error component of frequency-domain FOS signal, associated with the anisochronous (having amplitude-dependent period) vibrations, typical for vibration frequency-based sensors [21].

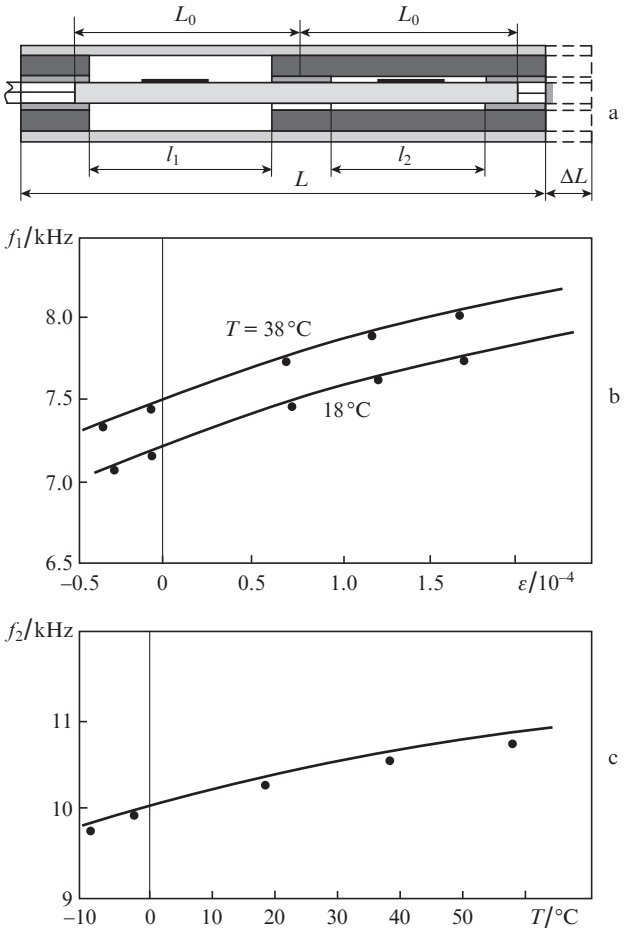

Figure 10. Schematic diagram of vibration frequency-based transducer of deformations and temperature on the base of SMS1 structure (a) and calibrating curves $f_1(\varepsilon, T)$ (b) and $f_2(T)$ (c); $\varepsilon = \Delta L/L$.

The performed studies of optical waveguide structures open the possibilities for creating multivariate vibration frequency-based FOSs, using the method of frequency division of measurement channels. Figure 11 shows a schematic diagram of the measuring transducer of such a sensor on the basis of a SMS, designed for simultaneous control of deformations ε and temperature T. The sensitive element of the transducer is the MMF segment, one section of which (l_1) is placed in the thin-walled part of the transducer housing, experiencing longitudinal deformations. Under these conditions the resonance frequency of the vibrating segment $f_1(\varepsilon, T)$ depends both on the deformations and on the temperature (Fig. 11b). The other section (l_2) is located in the massive thick-walled part of the housing, insensitive to longitudinal forces, and possesses the resonance frequency $f_2(T)$ (Fig. 11c). As a result, the measured values of f_1 and f_2 allow separate determination of deformation $\varepsilon(f_1, f_2)$ and temperature $T(f_2)$. Due to the high stability of physicochemical properties and perfect elastic and durable properties of the fibres made of uniform and pure silica glass, which are exploited in the proposed SMS structures, the considered vibration frequency-based FOSs may have large service life period (over 20 years) and high reliability under severe operation conditions.

19. Conclusions

The oscillation regimes in ELs, experiencing resonance interaction with microoptomechanical resonance structures of various types, are studied. In the case, when the MOMRS eigenfrequencies coincide with the frequencies of relaxation oscillations of intermode beats at EFL oscillation, the stable self-modulation regimes arise in the system, the modulation frequency being determined mainly by the eigenfrequency of the acoustomechanical MOMRS vibrations. These regimes may be implemented in a wide range of resonance frequencies and Q-factor values of the microoscillators with various mechanisms of photoinduced deformation excitation of the MOMRS vibrations. It should be noted that the MOMRS in the laser schemes may play the role of a complex passive modulator, implementing the modulation not only of the resonator Q-factor and light wave phase, but also of the polarisation anisotropy (modulated phase plate) and the frequency of light, reflected from the MOMRS, which essentially expands the variety of laser dynamic regimes.

The stabilisation of self-modulation frequency ($\Delta F/F \sim 10^{-5}$) may find application in laser radiation sources with high stability of pulse repetition rate. It is shown that using resonance modulation of FL pump is efficient for increasing the sensitivity of the laser in registration of small perturbations of the optical resonator characteristics. Due to the dependence of the MOMRS eigenfrequencies on the external conditions and perturbations, this phenomenon can be a basis for creating high-precision and noise-immune fibreoptic transducers and sensors of physical quantities with frequency output. We demonstrate the possibility to design multivariate measuring systems, based on the method of partial division of measurement channels, with miniature microoscillator sensor elements.

References

1. Hossein-Zaden M., Vahala K.J. *IEEE J. Sel. Top. Quantum Electron.*, **16** (1), 276 (2010).
2. Gorodetskii M.L. *Opticheskie mikroresonatory s gigantskoi dobrotnost'yu* (Optical Microresonators with a Giant *Q*-Factor) (Moscow: Fizmatlit, 2011).
3. Tsukanov M.L. *Mikroelektron.*, **40** (5), 359 (2011).
4. Varadan V.K., Vinoy K.J., Jose K.A. *RF MEMs and Their Applications* (Chichester: John Wiley & Sons, 2003).
5. Egorov F.A. *Avomodulyatsia intensivnosti lazernogo izlucheniya, vzaimodeystvuyushchego s mikrorezonatornymi strukturami. Avtoreferat kand. diss*. (Intensity Self-Modulation of Laser Radiation, Interacting with Microresonator Structures. Author's Abstract of Candidate of Sci. Thesis) (Moscow, 1997).
6. Yahel E., Hardy A. *J. Lighwave Technol.*, **21** (9), 2044 (2003).
7. Chartier T., Sauchez F., Stepfan G. *Appl. Phys. B*, **70**, 23 (2000).
8. Burkov V.D., Egorov F.A., Potapov V.T., Potapov T.V. *Radiotekh. Elektron.*, **45** (7), 880 (2000) [*Journal of Communications Technology and Electronics*, **45** (7), 797 (2000)].
9. Egorov F.A., Potapov V.T., Neugodnikov A.P., Nikitin V.V. *Vestnik Moskovskogo Univer., Ser. Fiz., Astronom.*, **64** (6), 45 (2009) [*Moscow University Physics Bulletin*, **64** (6), 605 (2009)].
10. Ambartsumyan R.V., Basov N.G., Kryukov P.G., Letokhov V.S. *Zh. Eksp. Teor. Fiz.*, **51** (3), 724 (1966) [*Sov. Phys. JETP*, **24** (3), 481 (1967)].
11. Ratner A.M. *Kvantovye generatory s bol'shim uglovym raskhozhdeniem* (Quantum Oscillators with Large Angle Divergence) (Kiev: Nukova Dumka, 1970).
12. Burkov V.D., Egorov F.A., Potapov V.T. *Pis'ma Zh. Tekh. Fiz.*, **23** (6), 33 (1997) [*Tech. Phys. Lett.*, **23** (3), 224 (1997)].
13. Burkov V.D., Egorov F.A., Potapov V.T. *Zh. Tekh. Fiz.*, **75** (1), 70 (2005) [*Tech. Phys.*, **50**, 69 (2005)].
14. Egorov F.A., Potapov V.T. *Pis'ma Zh. Tekh. Fiz.*, **35** (12), 104 (2009) [*Tech. Phys. Lett.*, **35** (9), 834 (2009)].
15. Babakov I.M. *Teoriya kolebanii* (Theory of Oscillations) (Moscow: Nauka, 1968).
16. Yariv A. *Quantum Electronics* (New York: Wiley Interscience, 1989).
17. Van Thourhout D., Roels J. *Nature Photon.*, **4**, 211 (2010).
18. Egorov F.A., Potapov V.T. *Pis'ma Zh. Tekh. Fiz.*, **36** (2), 86 (2010) [*Tech. Phys. Lett.*, **36** (6), 580 (2010)].
19. Snyder A.W., Love J.D. *Optical Waveguide Theory* (London: Chapman and Hall, 1983).
20. Veber A.A., Kurkov A.S., Tsvetkov V.B. *Laser Phys.*, **21** (2), 294 (2011).
21. Etkin L.G. *Vibrochastotnye datchiki. Teoriya i praktika* (Vibration Frequency-Based Sensors. Theory and Practice) (Moscow: Izd-vo MGTU im. N.E. Baumana, 2004).
22. Lisenkov I.V., Nikitov S.A., Popov R.S., Chul Koo Kim, *Radiotekh. Elektron.*, **52** (9), 1122 (2007) [*Journal of Communications Technology and Electronics*, **52** (9), 1037 (2007)].
23. Wiederhecker G.S., Brenn A., Fragnito H.L., Russell P.St.J. *Phys. Rev. Lett.*, **100**, 2003903 (2008).
24. Biryukov A.S., Sukharev M.E., Dianov E.V. *Kvantovaya Elektron.*, **32** (9), 765 (2002) [*Quantum Electron.*, **32** (9), 756 (2002)].
25. Egusa S., Wang Z., Chocat N., et al. *Nature Mater.*, **9**, 643 (2010).
26. Brambilla G., Xu F., Horak P., Jung Y., et al. *Adv. Opt. Photon.*, **1** (1), 107 (2009).
27. Egorov F.A., Nikitov S.A., Potapov V.T. *Radiotekh. Elektron.*, **50** (6), 736 (2005) [*Journal of Communications Technology and Electronics*, **50** (6), 673 (2005)].
28. Svetlitskiy V.A. *Mekhanika truboprovodov i shlangov* (Mechanics of Pipelines and Hoses) (Moscow: Mashinostroenie, 1982).
29. Nesterov S.V., Akulenko L.D., Korovina L.I. *Dokl. Ross. Akad. Nauk*, **427** (6), 781 (2009) [*Dokl. Phys.*, **54** (8), 402 (2009)].
30. Bolotin V.V. *Dinamicheskaya ustoychivost' uprugikh system* (Dynamical Stability of Elastic Systems) (Moscow: GITTL, 1956).
31. Verbridge S.S., Ilic R., Craighead H.G., Jeevak P.M. *Appl. Phys. Lett.*, **93**, 013101 (2008).
32. Biryukov A.S., Dianov E.M. *Kvantovaya Elektron.*, **37** (4), 379 (2007) [*Quantum Electron.*, **37** (4), 379 (2007)].
33. Ding Ye, Yang Q., Guo Xin, Wang S., et al. *Opt. Express*, **17** (24), 21813 (2009).
34. Luan F., George A.K., Knight J.C. *Opt. Express*, **15** (3), 829 (2007).
35. Braginsky V.B., Strigin S.E., Vyatchanin S.P. *Phys. Lett. A*, **287**, 331 (2001).
36. Maylybayev A.A. *Mnogoparametricheskie zadachi teorii ustoichivosti. Avtoreferat dokt. diss.* (Multiparametric Problems of Stability Theory. Author's Abstract of Doctor of Sci. Thesis) (St Petersburg, 2008).
37. Banerji J., Davies A.R., Jenkins R.M. *Opt. Soc. Am. B.*, **14** (9), 2378 (1997).
38. Frasao O., Silva S.O., Viegas J., et al. *Appl. Opt.*, **50** (25), E184 (2011).
39. Wu Q., Semenova Y., Wang P., Farrell G. *Proc. SPIE Int. Soc. Opt. Eng.*, **7753**, 77535G (2011).
40. Michtchenko A., Tulaikova T. *AIP Conf. Proc.*, **1253** (1), 254 (2010).
41. Born M., Wolf E. *Principles of Optics* (Cambridge University Press, 1999).
42. Lacot E., Jacquin O., Roussely G. et al. *J. Opt. Soc. Am. A*, **27** (11), 2450 (2010).
43. Arellano-Sotelo H., Kiryanov A.V., Barmenkov Yu.O., Aboites V. *Opt. Laser Technol.*, **43**, 132 (2011).
44. Witomski A., Lacot E., Hugon O. *Phys. Rev. A*, **72**, 023801 (2005).